



**HAL**  
open science

# Carbon Quantum Dot-Catalyzed, Highly Efficient Miniemulsion Atom Transfer Radical Polymerization Induced by Visible Light

Xiaoguang Qiao, Liang Qiao, Mengjie Zhou, Xi Zhang, Ge Shi, Yanjie He, Elodie Bourgeat-Lami, Xinchang Pang

► **To cite this version:**

Xiaoguang Qiao, Liang Qiao, Mengjie Zhou, Xi Zhang, Ge Shi, et al.. Carbon Quantum Dot-Catalyzed, Highly Efficient Miniemulsion Atom Transfer Radical Polymerization Induced by Visible Light. *ACS Macro Letters*, 2022, 11 (11), pp.1298-1305. 10.1021/acsmacrolett.2c00542. hal-03848738

**HAL Id: hal-03848738**

**<https://hal.science/hal-03848738v1>**

Submitted on 17 Nov 2022

**HAL** is a multi-disciplinary open access archive for the deposit and dissemination of scientific research documents, whether they are published or not. The documents may come from teaching and research institutions in France or abroad, or from public or private research centers.

L'archive ouverte pluridisciplinaire **HAL**, est destinée au dépôt et à la diffusion de documents scientifiques de niveau recherche, publiés ou non, émanant des établissements d'enseignement et de recherche français ou étrangers, des laboratoires publics ou privés.

1  
2  
3  
4 **Carbon Quantum Dots (CQDs) Catalyzed Highly Efficient**  
5  
6 **Miniemulsion Atom Transfer Radical Polymerization Induced by**  
7  
8 **Visible Light**  
9

10  
11 Xiaoguang Qiao,<sup>a,b§\*</sup> Liang Qiao,<sup>b§</sup> Mengjie Zhou,<sup>b</sup> Xi Zhang,<sup>b</sup> Ge shi,<sup>b</sup> Yanjie He,<sup>b</sup>  
12  
13 Bourgeat-Lami Elodie,<sup>c</sup> Xinchang Pang<sup>b\*</sup>  
14  
15  
16  
17  
18

19 <sup>a</sup>College of Materials Engineering, Henan International Joint Laboratory of Rare  
20 Earth Composite Materials, Henan Engineering Technology Research Center for  
21 Fiber Preparation and Modification, Henan University of Engineering, Zhengzhou, P.  
22 R. China, 451191  
23  
24  
25  
26  
27  
28

29 <sup>b</sup>Henan Joint International Research Laboratory of Living Polymerizations and  
30 Functional Nanomaterials, Henan Key Laboratory of Advanced Nylon Materials and  
31 Application, School of Materials Science and Engineering, Zhengzhou University,  
32 Zhengzhou 450001, China  
33  
34  
35  
36  
37  
38

39 <sup>c</sup>Univ. Lyon, Université Claude Bernard Lyon 1, CPE Lyon, CNRS, UMR 5128,  
40 Catalysis, Polymerization, Processes and Materials (CP2M), 43, Bvd. du 11  
41 Novembre 1918, 69616 Villeurbanne, France  
42  
43  
44  
45  
46

47 E-mail: [joexiaoguang@hotmail.com](mailto:joexiaoguang@hotmail.com)

48 [Pangxinchang1980@163.com](mailto:Pangxinchang1980@163.com)  
49  
50  
51  
52  
53  
54

55 [\*] To whom correspondence should be addressed.

56 [§] These authors contributed equally to this work.  
57  
58  
59  
60

**Abstract:**

Owing to the benefits of using natural or artificial light sources as a stimulus, photo-induced reversible-deactivation radical polymerization (photoRDRP) techniques have been recognized to be a powerful “green” platform for the preparation of well-defined polymers. However, the development of highly efficient visible light-induced photoRDRP processes in aqueous dispersed media remains a challenge due to light scattering and refraction by monomer droplets or colloidal particles. In this work, an efficient green photocatalyst, carbon quantum dots (CQDs), was introduced to visible light-mediated miniemulsion atom transfer radical polymerization (ATRP), leading to highly efficient polymerizations with reaction rates (>80% monomer conversion within 1h) much higher than in previous studies. This heterogeneous photocatalytic system is presumed to involve three catalytic cycles in: i) the aqueous phase, ii) the oil-water interface and iii) the monomer droplets. The effect of different polymerization parameters on the polymerization reaction was investigated, including the amounts of surfactant and CQDs,  $\text{CuBr}_2$  dosage and solid content. Excellent temporal control of the polymerization was illustrated by “ON/OFF” polymerizations, and natural sunlight was also used as an energy source. This novel CQDs-catalyzed miniemulsion photoATRP process may be easily extended to other aqueous dispersion RDRP systems. As an extension of our previous work (*J. Am. Chem. Soc.* 2022, 144, 22, 9817–9826) we also developed a “one-pot” method for the rapid preparation of heterogeneous hydrogels.

## Introduction

According to the principles of green polymerization, the ideal polymerization reaction is one that quantitatively converts monomers into well-defined polymers, with maximize economy and reduce waste.<sup>1,2</sup> In this regard, photomediated reversible-deactivation radical polymerizations (photoRDRP), using in particular visible light as a “green” energy source, have attracted broad research interest.<sup>3,4</sup> In addition, photoRDRP can be carried out in aqueous media, which is particularly relevant from an environmental perspective, offering better temperature control due to easy heat removal, and leading to high solids, low viscosity polymers.<sup>5,6</sup> Polymerizations in aqueous dispersed media encompass a variety of processes including miniemulsion, emulsion, suspension and dispersion polymerization, all of which are used extensively in many applications.<sup>5,7-9</sup>

PhotoRDRP techniques including atom transfer radical polymerization (ATRP) and reversible addition–fragmentation chain transfer (RAFT) have been widely developed in miniemulsion.<sup>10-12</sup> In contrast to the high-energy UV irradiation which may lead to photodegradation of the photoinitiator or to undesirable side reactions, milder visible light is expected to remedy most of these drawbacks.<sup>13,14</sup> The first reported technique for visible light-induced photoRDRP in miniemulsion was photo-induced electron transfer-RAFT (PET-RAFT).<sup>12,15,16</sup> PET-RAFT was used to mediate the controlled polymerization of styrene in an oil-in-water (O/W) miniemulsion by using blue light ( $\lambda = 460$  nm) as a stimulus and Ir(ppy)<sub>3</sub> as photocatalyst. However, depletion of the photocatalyst from the oily monomer droplets during polymerization, led to low

1  
2  
3  
4 reaction rates and limiting conversions. The same group then developed RAFT  
5  
6 iniferter miniemulsion polymerization under green light irradiation ( $\lambda = 530$  nm),  
7  
8 based on light-induced photolysis of the RAFT agent.<sup>16</sup> However, despite obvious  
9  
10 progress in RAFT polymerization, UV light still remains the dominant source in the  
11  
12 case of miniemulsion photoATRP.<sup>10,11</sup> Matyjaszewski and coworkers reported the UV  
13  
14 light-mediated photoATRP of (meth)acrylic monomers in miniemulsion, and  
15  
16 demonstrated the efficient control of polymerization through the formation of an  
17  
18 ion-pair catalyst by interaction of the Cu/ligand with sodium dodecyl sulfate (SDS).<sup>10</sup>  
19  
20 This ion-pair photoATRP catalytic system was next successfully extended to more  
21  
22 industrially relevant ab initio emulsion polymerization.<sup>11</sup> However, accessing high  
23  
24 reactivity under mild visible light irradiation in aqueous dispersed media remains a  
25  
26 challenge in photoATRP. One main reason is the opacity of the aqueous dispersion  
27  
28 system, and the light scattering and refraction contribute to radiation attenuation.<sup>17</sup> In  
29  
30 this respect, the use of highly efficient photocatalysts appears to be a promising  
31  
32 approach to address this problem.  
33  
34  
35  
36  
37  
38  
39  
40  
41  
42

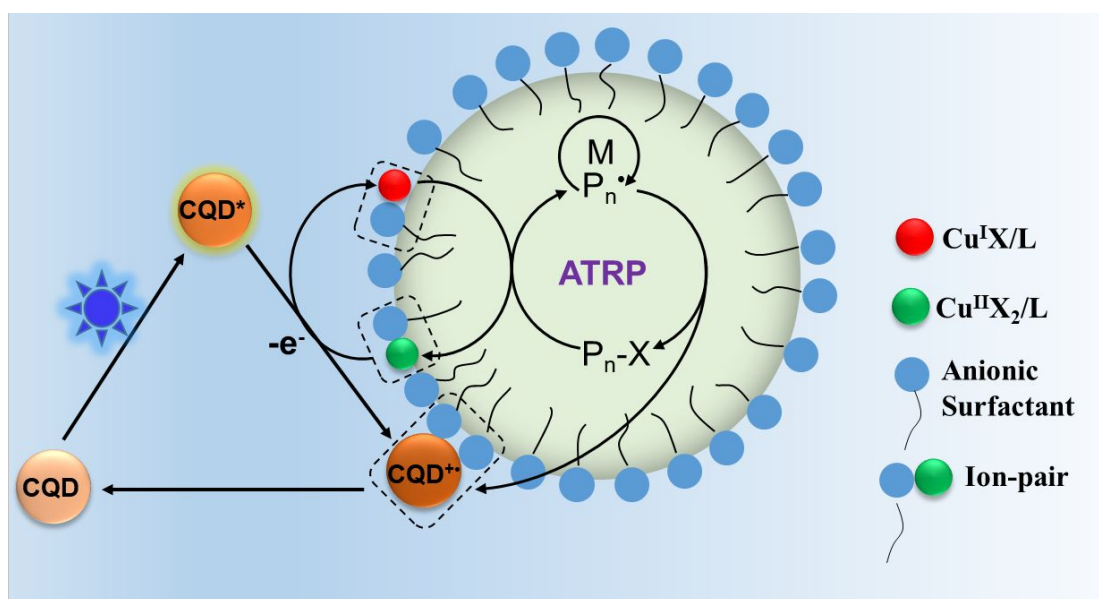
43 In this paper, a highly efficient visible light-induced miniemulsion ATRP system is  
44  
45 developed for the first time by using pyridine nitrogen-doped carbon dot (CQDs) as  
46  
47 photocatalyst. Higher than 80% monomer conversion could be achieved within 1h,  
48  
49 with a good control of polymer molecular weights and low dispersities ( $M_w/M_n <$   
50  
51 1.20). Several parameters were explored, including the concentrations of surfactant,  
52  
53 copper catalyst and CQDs as well as the solids content. In addition, the temporal  
54  
55 control of polymerization was achieved by switching the blue light “ON” and “OFF”,  
56  
57  
58  
59  
60

1  
2  
3  
4 and polymerization could also be carried out with natural sunlight. As an extension of  
5  
6 our previous work,<sup>16</sup> we also developed a “one-pot” method for the rapid preparation  
7  
8 of heterogeneous hydrogels.  
9

## 10 11 **Results and discussion**

12  
13  
14 Due to their low toxicity, easy preparation, sustainability of raw materials, stable  
15  
16 optical properties and other advantages, CQDs have been recently reported to be ideal  
17  
18 green photocatalysts for both photoATRP and PET-RAFT.<sup>18-21</sup> Notably, our group  
19  
20 developed an ultrafast visible light-induced ATRP system in aqueous media with  
21  
22 100% pyridine nitrogen-doped CQDs as the catalyst, which can be further applied for  
23  
24 digital light processing 3D printing.<sup>18,21</sup> The ultrafast polymerization rate was  
25  
26 attributed to the combination of excellent catalytic capacity, a high equilibrium  
27  
28 constant,  $K_{\text{ATRP}}$ , for Cu-catalyzed ATRP and a high rate of electron transfer in  
29  
30 aqueous media.<sup>22,23</sup> Additionally, the abundant surface groups enabled CQDs to be  
31  
32 well dispersed in aqueous media and the large surface area enhanced contact between  
33  
34 CQDs and the  $\text{Cu}^{\text{I}}\text{X}/\text{L}$  complex.<sup>24</sup> According to this, we anticipate that N-doped  
35  
36 CQDs may be a suitable heterogeneous photocatalyst for miniemulsion photoATRP.  
37  
38 The photocatalyst is expected to work in synergy with the ATRP ion-pair catalyst,  
39  
40 provoking a cascade of photocatalytic reactions taking place in the water phase, the  
41  
42 oil-water interface and the monomer droplets, respectively. As described in Scheme 1,  
43  
44 the formed monomer droplets after ultra-sonicating are stabilized by the anionic  
45  
46 surfactant SDS. According to pioneer works,<sup>10,25</sup> the  $\text{Cu}^{\text{I}}\text{X}_2/\text{L}$  complex can form  
47  
48 ion-pair with the surfactant molecules at the oil-water interface. Upon visible light  
49  
50  
51  
52  
53  
54  
55  
56  
57  
58  
59  
60

1  
2  
3  
4 irradiation, CQDs in the water phase can form electron-hole pairs and act as excellent  
5  
6 electron donors.<sup>18,26</sup> With the help of water, which can stabilize the charge separated  
7  
8 species, electrons can quickly transfer from excited  $CD^*$  to the  $Cu^{II}X_2/L$  complex  
9  
10 resulting in the formation of  $Cu^I X/L$  complex. The resulting hydrophobic  
11  
12  $Cu^I X/L/SDS$  ion pair complex later can then enter the monomer droplets and undergo  
13  
14 a catalytic ATRP cycle with the alkyl bromide as the initiator. The CQDs that lose  
15  
16 electrons have a positive surface charge ( $CD^{*+}$ ), and can thus adsorb onto the  
17  
18 negatively charged monomer droplets by electrostatic interaction. As an electron  
19  
20 acceptor, the oxidized  $CD^{*+}$  can be involved in promoting dormancy of living polymer  
21  
22 chains,<sup>20,21</sup> and go back to the ground state,  $CD$ , which may escape to the water phase  
23  
24 from the oil/water interface (Scheme 1).  
25  
26  
27  
28  
29  
30  
31



Scheme 1. Proposed mechanism for CQDs-catalyzed visible light-induced miniemulsion ATRP.

Table 1. Experimental conditions and results of CQDs-catalyzed photoinduced miniemulsion ATRP reactions performed in this study.<sup>a</sup>

Entry	$[M]_0:[RX]_0:[Cu]_0:[L]_0$	SDS (wt%)	CQDs (mg/mL)	Cu concentration (ppm)	Solids content (wt%)	Time (min)	$\alpha$ (%)	$M_{n,th}^b$	$M_{n,SEC}^c$	$M_w/M_n^c$	$Z_{av.} (nm)^d$	PDI
1	200:1:0.06:0.36	2.5	0.4	300	20	60	48	12500	12780	1.54	190	0.06
2	200:1:0.06:0.36	5.0	0.4	300	20	60	72	18600	15100	1.21	160	0.04
3	200:1:0.06:0.36	10.0	0.4	300	20	60	81	21000	21000	1.21	104	0.07
4	200:1:0.02:0.12	10.0	0.4	100	20	60	84	21700	19100	1.33	109	0.06
5	200:1:0.12:0.72	10.0	0.4	600	20	60	69	17960	15630	1.17	104	0.08
6	200:1:0.06:0.36	10.0	0.2	300	20	60	72	18700	17300	1.19	106	0.05
7	200:1:0.06:0.36	10.0	0.8	300	20	60	77	19980	20100	1.20	92	0.05
8	200:1:0.06:0.36	10.0	0.4	300	10	60	71	18300	16530	1.23	103	0.04
9	200:1:0.06:0.36	10.0	0.4	300	30	60	72	18580	15210	1.20	95	0.06
10 <sup>e</sup>	200:1:0.06:0.36	10.0	0.4	300	20	60	89	25500	22580	1.38	108	0.09

<sup>a</sup>Reaction conditions:  $[M]/[RX]/[Cu]/[L] = [BA]/[EBiB]/[CuBr_2]/[TPMA]$ , 460 nm irradiation (6W) at room temperature.  $V_{tot} = 5$  mL. Stirring rate = 500 rpm.

<sup>b</sup>Theoretical molecular weight calculated according to:  $M_{n,th.} = [M]_0/[RX]_0 \times MW^M \times \alpha + MW^{RX}$ , where  $[M]_0$ ,  $[RX]_0$ ,  $MW^M$ ,  $\alpha$ , and  $MW^{RX}$  correspond to initial monomer concentration, initial RX concentration, molar mass of monomer, conversion determined by gravimetric analysis, and molar mass of alkyl halide. <sup>c</sup>Number average molecular weight and dispersity determined by SEC analysis (DMF as eluent) calibrated with polystyrene standard. <sup>d</sup>Final average hydrodynamic particle diameter determined by DLS. <sup>e</sup>Monomer = BMA.



1  
2  
3  
4 The polymerization of *n*-butyl acrylate (BA) was initially investigated to test the  
5  
6 efficiency of our visible light-mediated miniemulsion ATRP process, using blue light  
7  
8 ( $\lambda = 460$  nm,  $2\text{mW}/\text{cm}^2$ ) as the irradiation. Pyridine nitrogen-doped CQDs were  
9  
10 prepared as reported previously.<sup>18,21</sup> In a typical reaction (Table S1), ethyl  
11  
12  $\alpha$ -bromoisobutyrate (EBiB) was used as alkyl halide initiator together with ppm level  
13  
14 of the  $\text{CuBr}_2/\text{tris}(2\text{-pyridylmethyl})\text{amine}$  (TPMA) complex ( $[\text{CuBr}_2]:[\text{TPMA}] = 1:6$ ).  
15  
16 As listed in Table 1 (entries 1-3), the amount of SDS was varied from 2.5 to 10.0 wt%  
17  
18 based on monomer, while the CQD and copper salt concentrations were held constant  
19  
20 (0.4 mM and 300 ppm, respectively). Notably, the polymerization performed using 10  
21  
22 wt% of SDS achieved 81% monomer conversion within 1h, which polymerization  
23  
24 rate is significantly higher than in previous reports (see Table S2 in the Supporting  
25  
26 Information). In addition, molecular weights were in very good agreement with the  
27  
28 theoretical values while SEC analysis indicated a narrow molecular weight  
29  
30 distribution ( $D = 1.21$ , entry 3 in Table 1) suggesting a good level of control. In  
31  
32 contrast, lower amounts of SDS led to lower monomer conversions within the same  
33  
34 reaction period, and to larger particles (Table 1 and Figure S1). Moreover, a relatively  
35  
36 higher polydispersity ( $D = 1.54$ ) was observed for the reaction performed using 2.5  
37  
38 wt% of SDS. As increasing SDS concentration resulted in smaller (and therefore  
39  
40 larger number concentration) monomer droplets, a higher polymerization rate was  
41  
42 achieved in agreement with the so-called segregation effect (compartmentalization)  
43  
44 that is well documented in the case of miniemulsion RDPR, leading to a reduction in  
45  
46 the rate of bimolecular termination.<sup>27</sup> Moreover, the decrease of SDS concentration  
47  
48  
49  
50  
51  
52  
53  
54  
55  
56  
57  
58  
59  
60

1  
2  
3  
4 resulted in low concentration of  $\text{Cu}^{\text{I}}\text{X}_2/\text{L}/\text{SDS}$  ion pair complex, and reduced the  
5  
6 copper catalyst involved in ATRP. Together with the so-called confined space effect  
7  
8 (compartmentalization),<sup>27</sup> the larger size of droplets (or particles) induced by much  
9  
10 lower SDS concentration would result in the loss control of polydispersity.  
11  
12

13  
14 For all three SDS concentrations, the corresponding semi-logarithmic plot of  
15  
16  $\text{Ln}([\text{M}]_0/[\text{M}]_t)$  versus time indicates two distinct linear regimes (see Figure 1a). The  
17  
18 first regime corresponds to a “fast” polymerization followed by a decrease in reaction  
19  
20 rate. According to the interfacial “ion-pair catalysis” mechanism of Scheme 1, one  
21  
22 possible explanation for this “two stages” kinetic behavior is the drastic change of the  
23  
24 internal viscosity of the monomer droplets with time. The viscosity inside the  
25  
26 monomer droplets or latex particles increases with increasing monomer conversion  
27  
28 and molecular weights, which may limit the rotation and movement of the dormant  
29  
30 chains ( $\text{P}_n\text{-X}$ ) and propagating radicals ( $\text{P}_n\cdot$ ). According to the RDRP polymerization  
31  
32 mechanism, most of the polymer chains should be in a dormant state to achieve the  
33  
34 controlled growth of polymer chains. The contact between  $\text{Cu}^{\text{I}}\text{X}/\text{L}$  complex and  $\text{P}_n\text{-X}$   
35  
36 likely became difficult as diffusion was hindered due to the high viscosity for high  
37  
38 monomer conversions, leading to a decrease in the concentration of propagating  
39  
40 radicals (Figures 1b and 1c). A closer observation showed that  $M_{n, \text{SEC}}$  became slightly  
41  
42 lower than the theoretical value for high monomer conversion with less SDS  
43  
44 concentrations (Figure 1b). Although the overall concentration of propagating radicals  
45  
46 was decreased for high viscosity, the activation period of propagating radicals may  
47  
48 increase in limited region, due to the limitation of dormancy and termination which  
49  
50  
51  
52  
53  
54  
55  
56  
57  
58  
59  
60

also controlled by diffusion. Degradation reaction may occur in such limited region, resulting in a slightly lower molecular weight of the polymer than the theoretical value. In view of the confined space effect, the system with higher SDS content and small particle size may reduce the occur probability of degradation reaction.<sup>27</sup>

Nonetheless, all SEC traces were unimodal and shifted toward higher molecular weights with increasing monomer conversion, indicating reasonably good control over the polymerization up to high conversions (Figure S2).

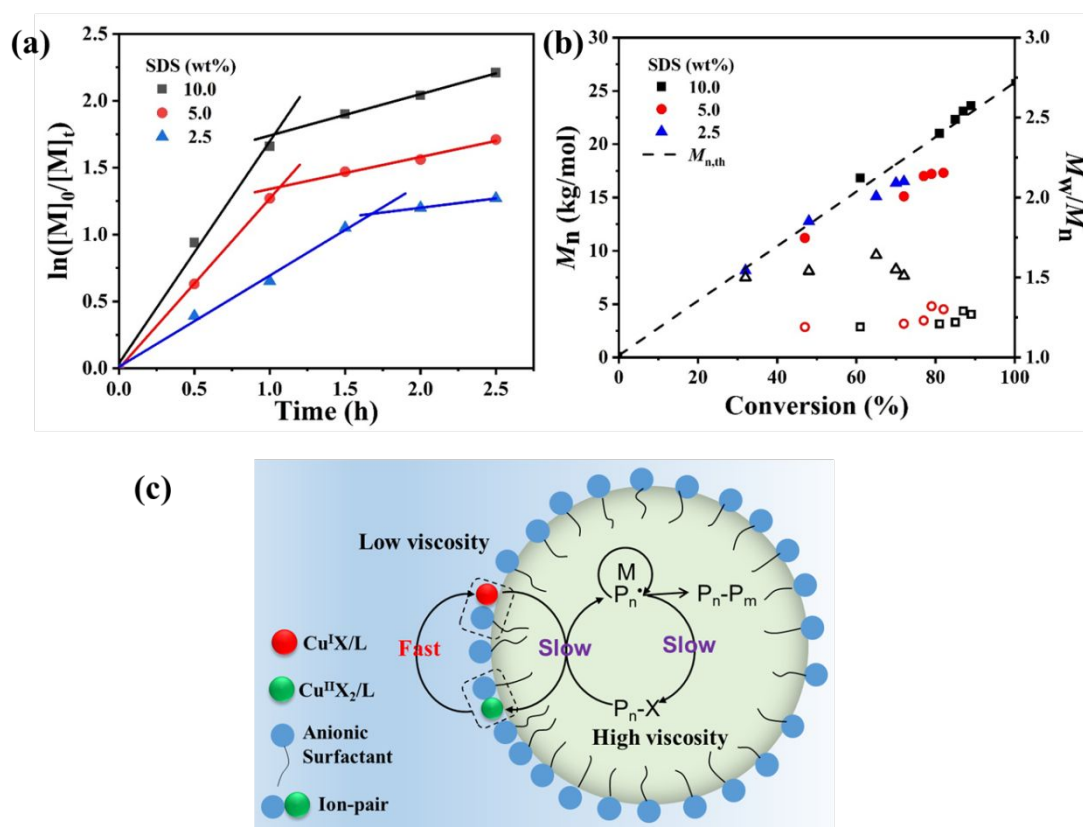


Figure 1. Influence of the SDS concentration on the CQDs-catalyzed miniemulsion photoATRP of BA. a) Kinetic plot of  $\ln([M]_0/[M]_t)$  versus exposure time, b) evolution of  $M_n$  and  $M_w/M_n$  with conversion and c) proposed reaction mechanism. Reaction conditions: BA = 1 mL (20 vol %),  $[BA]/[EBiB]/[CuBr_2]/[TPMA] = 200/1/0.06/0.36$ ,  $[HD] = 10$  wt% relative to BA,  $[SDS] = 2.5$ – $10.0$  wt % relative to BA, CQDs = 0.4 mg/mL, blue LED irradiation (6 W,  $\lambda_{max} = 460$  nm, 2 mW  $cm^{-2}$ ), room temperature.

As shown in Figures 2a and 2b, the polymerization rate decreased with increasing

CuBr<sub>2</sub>/TPMA catalyst loading (entries 4, 3 and 5 in Table 1) due to the increased number of dormant active species. The quality of the control was therefore improved, as attested by the decrease of the molecular weight distributions. By comparison, the other parameters had a relatively minor effect on the polymerization rate as shown in Table 1 and Figure 2c-f. Indeed the droplet or particle sizes were only little influenced by the amount of CQDs or solids content (Table 1, Figure S4 and S6).<sup>28,29</sup>

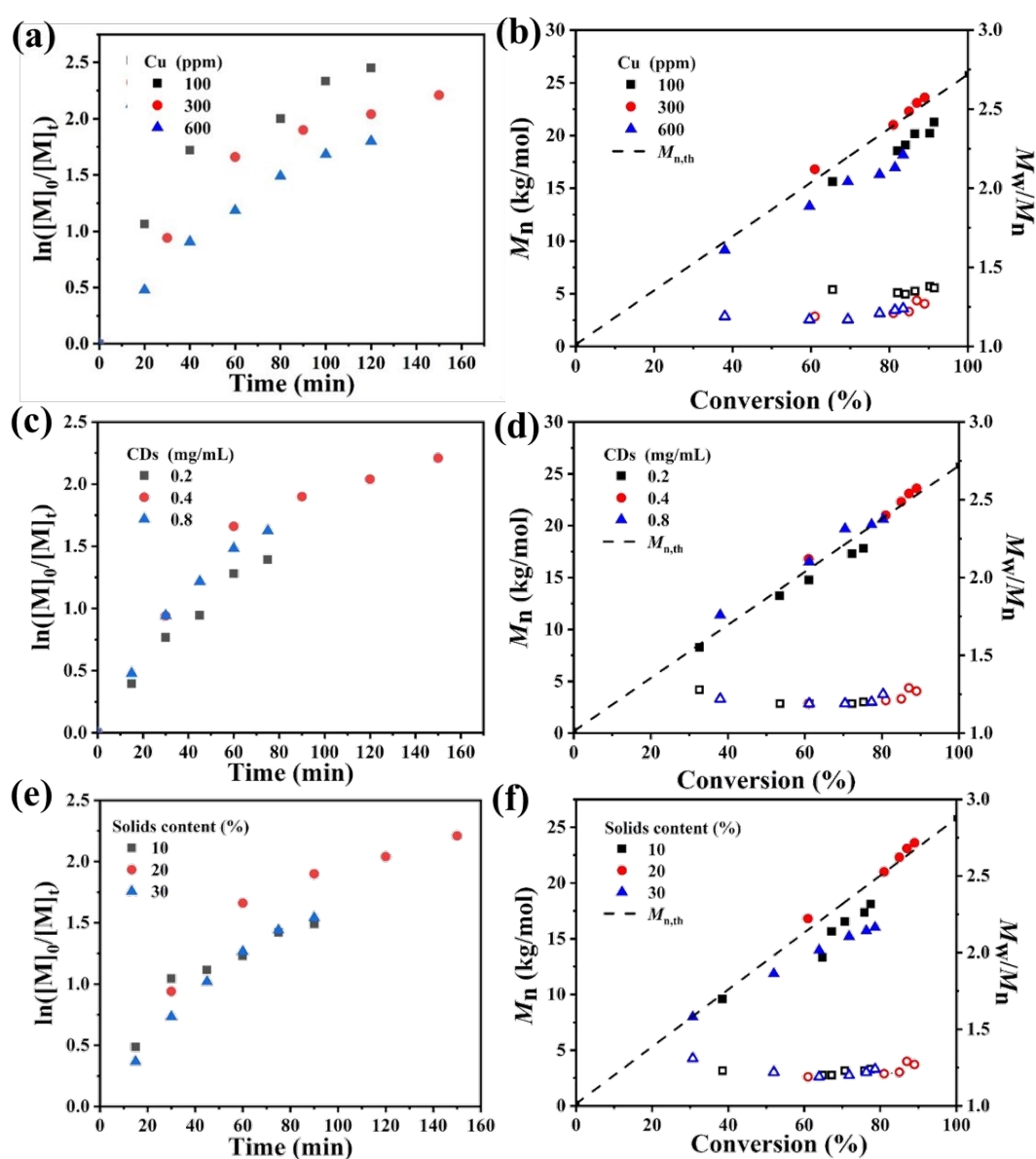


Figure 2. Effects of copper, CD and solids contents on CQDs-catalyzed miniemulsion photoATRP

1  
2  
3  
4 of BA under blue LED irradiation (6 W,  $\lambda_{\text{max}} = 460 \text{ nm}$ ,  $2 \text{ mW cm}^{-2}$ ) at room temperature. BA =  
5  
6 1 mL (20 vol %),  $[\text{BA}]/[\text{EBiB}] = 200/1$ ,  $[\text{HD}] = 10 \text{ wt \%}$  relative to BA,  $[\text{SDS}] = 10.0 \text{ wt \%}$   
7  
8 relative to BA. (a, c, e) Kinetic plot of  $\ln([\text{M}]_0/[\text{M}]_t)$  versus exposure time and (b, d, f) Evolutions  
9  
10 of  $M_n$  and  $M_w/M_n$  with monomer conversion.  
11  
12  
13  
14  
15

16 Subsequently, the experimental conditions of entry 1 in Table 1 were used to assess  
17  
18 the temporal control of CQDs-catalyzed miniemulsion photoATRP under blue LED  
19  
20 irradiation, by switching the light source “ON” and “OFF” with 15 min intervals  
21  
22 (Figure 3a). As expected, the polymerization stopped quickly when the light was  
23  
24 turned “OFF”, and recovered rapidly after switching it “ON”. The molar mass ( $M_n$ ,  
25  
26  $M_n^{\text{SEC}}$ ) did not change much during the “OFF” period, and increased after the light has  
27  
28 been switched “ON” to reach a value in good agreement with the theoretical  
29  
30 molecular weight ( $M_{n,\text{th}}$ ). The total exposure time was 45 min and a final PBA  
31  
32 polymer with a molar mass of  $19900 \text{ g mol}^{-1}$  and a low dispersity ( $M_w/M_n = 1.19$ )  
33  
34 could be successfully obtained. A purified PBA macroinitiator ( $M_n = 8500$ ,  $M_w/M_n =$   
35  
36  $1.22$ ) obtained through miniemulsion photoATRP was applied in another  
37  
38 miniemulsion photoATRP to confirm the chain-end fidelity. The PBA macroinitiator  
39  
40 was chain extended after well dissolved in BA monomer. As shown in Figure 3c,  
41  
42 well-defined PBA-*b*-PBA ( $M_n = 22500$ ,  $M_w/M_n = 1.19$ ) was achieved, evidenced by a  
43  
44 clear shift of the monomodal GPC traces toward higher molecular weights. The  
45  
46 polymerization was also carried on under natural sunlight as shown in Figure 3d.  
47  
48  
49  
50  
51  
52  
53  
54  
55  
56  
57  
58 After 1.5h, the monomer conversion reached 92% leading to stable PBA latex  
59  
60

particles with a molar mass of  $18700 \text{ g mol}^{-1}$  and again a narrow molecular weight distribution ( $M_w/M_n = 1.20$ ). Therefore, it can be concluded that the CQDs-catalyzed miniemulsion photoATRP maintains high polymerization efficiency, polymerization stability and good controllability even under natural sunlight source. BMA was also tested as another monomer in the same conditions (entry 10 in Table 1, Figure S7) leading to high monomer conversion ( $\sim 89\%$ ) within 1h, and reasonably good control illustrating the robustness and versatility of the process.

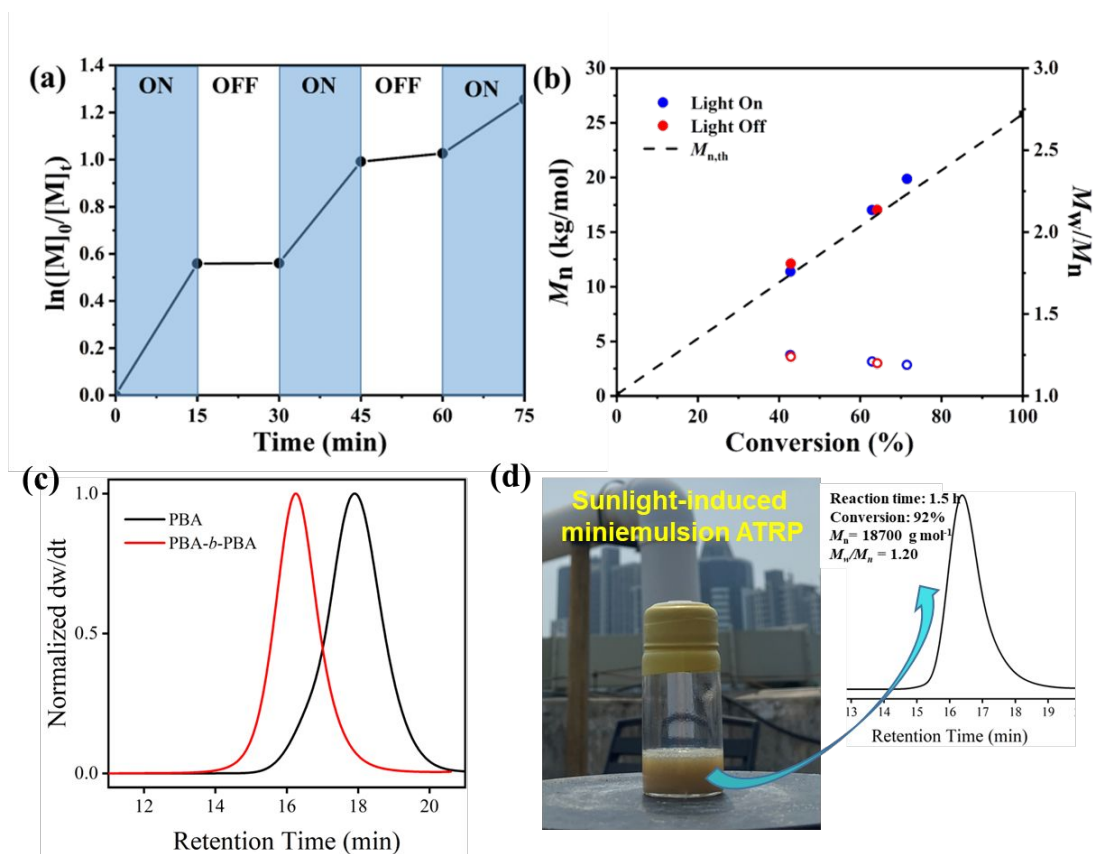


Figure 3. Temporal control of miniemulsion photoATRP. (a) Kinetic plot of  $\ln([M]_0/[M]_t)$  versus exposure time during “ON” and “OFF” periods and (b)  $M_n$  and  $M_w/M_n$  plots versus conversion during “ON” and “OFF” periods. (c) Chain extension of PBA macroinitiator with BA in miniemulsion. (d) Photo of sunlight-induced miniemulsion ATRP and SEC chromatogram of the final polymer. Reaction conditions: BA 1 mL (20 vol %),  $[BA]/[EBiB]/[CuBr_2]/[TPMA] = 200/1/0.06/0.36$ ,  $[HD] = 10 \text{ wt\%}$  relative to BA,  $[SDS] = 10 \text{ wt\%}$  relative to BA, CQDs = 0.4

1  
2  
3 mg/mL, blue LED irradiation (6 W,  $\lambda_{\text{max}} = 460 \text{ nm}$ ,  $2 \text{ mW cm}^{-2}$ ), room temperature.  
4  
5  
6  
7

8 We also developed a “one-pot” method for rapid preparation of heterogeneous  
9 hydrogels. The application of RDRP in preparation of polymer networks can not only  
10 bring more homogenous network, but also enable the production of “living” materials  
11 containing dormant reactivatable species which can be used for post  
12 functionlization.<sup>30</sup> The miniemulsion was prepared as described above using BA as  
13 hydrophobic monomer. After ultrasonic treatment, an hydrophilic monomer (HEA), a  
14 crosslinker polyethylene glycol diacrylate (PEGDA) and HEBiB initiator were added  
15 to the miniemulsion, followed by the addition of  $\text{CuBr}_2/\text{TPMA}$  and CQDs.  
16 PhotoATRP was performed simultaneously in the aqueous phase and within the  
17 hydrophobic monomer droplets under blue LED irradiation leading to an  
18 heterogeneous hydrogel composed of polymer particles embedded in a crosslinked  
19 water-swollen polymer network (Figure 4a). A digital image of the resulting  
20 heterogeneous hydrogel is depicted in Figure 4b (right) and compared to that of an  
21 homogeneous gel (left side of the Figure) obtained in similar conditions, using pure  
22 water as reaction medium instead of the miniemulsion. As expected, the  
23 heterogeneous hydrogel was less transparent due to light scattering by the PBA latex  
24 particles. In addition, the CQDs-containing hydrogel was endowed with  
25 photoluminescence characteristics.  
26  
27  
28  
29  
30  
31  
32  
33  
34  
35  
36  
37  
38  
39  
40  
41  
42  
43  
44  
45  
46  
47  
48  
49  
50  
51  
52  
53  
54  
55  
56  
57  
58  
59  
60

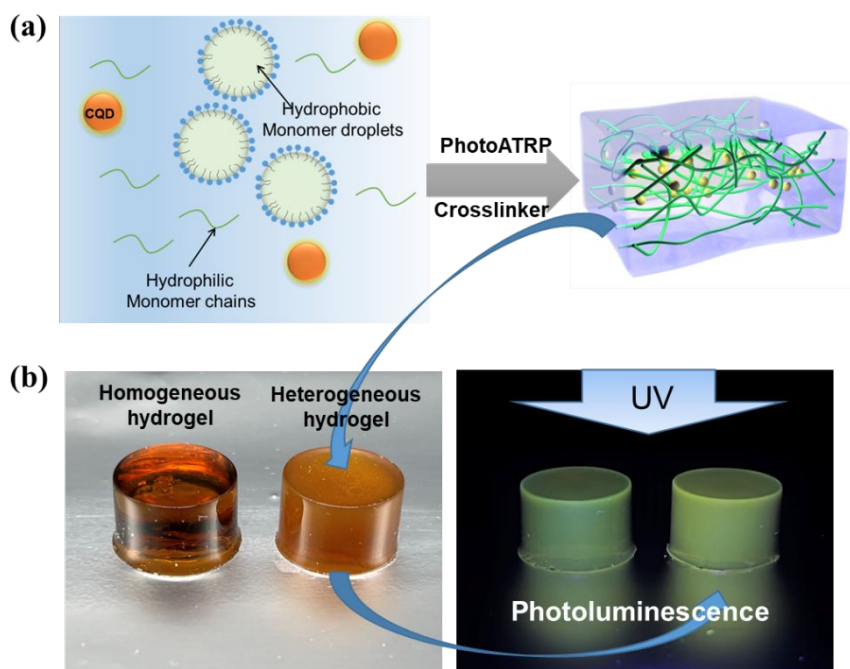


Figure 4. (a) Scheme for the preparation of heterogeneous hydrogels through CQDs-catalyzed photoATRP. (b) Digital photographs of homogeneous and heterogeneous hydrogels exposed to natural and UV light irradiations, respectively. Reaction conditions: BA 1 mL (20 vol %),  $[BA]/[EBiB]/[CuBr_2]/[TPMA] = 200/1/0.06/0.36$ ,  $[HD] = 10$  wt % relative to BA,  $[SDS] = 10$  wt % relative to BA, CQDs = 0.4 mg/mL,  $[HEA]/[PEGDA]/[HEBiB]/[CuBr_2]/[TPMA] = 90/10/1/0.03/0.18$ , blue LED irradiation (6 W,  $\lambda_{max} = 460$  nm,  $2 \text{ mW cm}^{-2}$ ), room temperature.

## Conclusions

In summary, we have shown that pyridine N-doped CQDs are excellent photocatalysts for visible light-induced miniemulsion ATRP, and are able to address the low efficiency problem of photoATRP in aqueous dispersed systems. The experimental results presented here suggest a heterogeneous interfacial photocatalytic mechanism involving three catalytic cycles in the water phase, the oil-water interface and the monomer droplets. In addition to the good control of polymerization, this novel CQDs-catalyzed miniemulsion photoATRP process allowed to reach very high



1  
2  
3  
4 monomer conversions (>80%) within 1h, which represents a significant advance in  
5  
6 the field. Excellent temporal control of the polymerization was illustrated by  
7  
8 “ON/OFF” polymerization, and natural sunlight was also exploited as harmful power  
9  
10 source. Moreover, photoATRP was successfully carried out simultaneously in an  
11  
12 aqueous phase and hydrophobic monomer droplets to prepare a heterogeneous  
13  
14 hydrogel in “one-pot”. Such hydrogels may find great potential as drug delivery  
15  
16 systems for biomedical applications. Owing to its efficiency and robustness, this new  
17  
18 CQDs-based photocatalytic platform should be suitable for other photoRDRP systems  
19  
20 opening the route to the synthesis of new particles and/or materials with obvious  
21  
22 economic and environmental benefits.  
23  
24  
25  
26  
27  
28  
29

## 30 **ASSOCIATED CONTENT**

### 31 **Supporting Information**

32  
33  
34 The Supporting Information is available free of charge on the ACS Publications  
35  
36 website, including brief description of materials, equipment used throughout the  
37  
38 experiment, experimental procedures for preparation and characterization of all  
39  
40 compounds.  
41  
42  
43  
44  
45  
46  
47

## 48 **AUTHOR INFORMATION**

### 49 **Corresponding Author**

50  
51 \*joexiaoguang@hotmail.com

52  
53  
54 \*Pangxinchang1980@163.com

### 55 56 57 58 59 **Author Contributions**

1  
2  
3  
4 §These authors contributed equally.  
5

6  
7 **Notes**  
8

9 The authors declare no competing financial interests.  
10

11  
12 **ACKNOWLEDGMENT**  
13

14  
15 The work was financially supported by National Science Foundation of China  
16 (Grant No.51973201, U1804128, 52173209), the National Science Foundation for  
17 Young Scientists of China (Grant No. 22105179) and Scientific & technological  
18 research projects in Henan Province (Grant No. 222102520009).  
19  
20  
21  
22  
23  
24  
25  
26  
27

28  
29 **REFERENCES**  
30

- 31 1. Dworakowska, S.; Lorandi, F.; Gorczyński, A.; Matyjaszewski, K. Toward Green  
32 Atom Transfer Radical Polymerization: Current Status and Future Challenges.  
33 Adv. Sci. 2022, 2106076.  
34  
35  
36  
37  
38 2. Huang, S.; Wang, H.; Ahmad, W.; Ahmad, A.; Ivanovich Vatin, N.; Mohamed, A.  
39 M.; Deifalla, A. F.; Mehmood, I. Plastic Waste Management Strategies and Their  
40 Environmental Aspects: A Scientometric Analysis and Comprehensive Review.  
41 Int. J. Env. Res. Public Health 2022, 19, 4556.  
42  
43  
44  
45  
46  
47  
48 3. Pan, X.; Tasdelen, M.A.; Laun, J.; Junkers, T.; Yagci, Y.; Matyjaszewski K.  
49 Photomediated Controlled Radical Polymerization. Prog. Polym. Sci. 2016, 62,  
50 73-125.  
51  
52  
53  
54 4. Corrigan, N.; Jung, K.; Moad, G.; Hawker, C. J.; Matyjaszewski, K.; Boyer, C.,  
55 Reversible-deactivation Radical Polymerization (Controlled/living Radical  
56 Polymerization): From Discovery to Materials Design and Applications. Prog.  
57  
58  
59  
60

- 1  
2  
3 Polym. Sci. 2020, 111, 101311.  
4  
5  
6 5. Cunningham, M.F. Controlled/Living Radical Polymerization in Aqueous  
7  
8 Dispersed Systems. Prog. Polym. Sci. 2008, 33, 365-398.  
9  
10  
11 6. Zetterlund, P.B.; Thickett, S.C.; Perrier, S.; Bourgeat-Lami, E.; Lansalot, M.  
12  
13 Controlled/Living Radical Polymerization in Dispersed Systems: An Update.  
14  
15 Chem. Rev. 2015, 115, 9745-9800.  
16  
17  
18 7. Qiu, J; Charleux, B; Matyjaszewski, K. Controlled/living radical polymerization  
19  
20 in aqueous media: homogeneous and heterogeneous systems. Prog. Polym. Sci.  
21  
22 2001, 26, 2083-2134.  
23  
24  
25  
26 8. Min, K.; Matyjaszewski, K. Atom transfer radical polymerization in aqueous  
27  
28 dispersed media. Open Chemistry, 2009, 7, 657-674.  
29  
30  
31  
32 9. Sanders, C.A.; Cunningham, M.F. Polymerizations in Aqueous Dispersed Media.  
33  
34 Macromolecular Engineering, 2022  
35  
36  
37 10. Wang, Y.; Dadashi-Silab, S.; Matyjaszewski, K. Photoinduced miniemulsion atom  
38  
39 transfer radical polymerization. ACS Macro Letters, 2018, 7, 720-725.  
40  
41  
42 11. Wang, Y.; Dadashi-Silab, S.; Lorandi F.; Matyjaszewski, K. Photoinduced atom  
43  
44 transfer radical polymerization in ab initio emulsion. Polymer, 2019, 165,  
45  
46 163-167.  
47  
48  
49 12. Xu, J.; Jung, K.; Boyer, C. Oxygen tolerance study of photoinduced electron  
50  
51 transfer–reversible addition–fragmentation chain transfer (PET-RAFT)  
52  
53 polymerization mediated by Ru(bpy)<sub>3</sub>Cl<sub>2</sub>. Macromolecules, 2014, 47, 4217-4229.  
54  
55  
56 13. Vogel, A.; Venugopalan, V. Mechanisms of Pulsed Laser Ablation of Biological  
57  
58 Tissues. Chem. Rev. 2003, 103, 577-644.  
59  
60

- 1  
2  
3  
4 14. Corrigan, N.; Yeow, J.; Judzewitsch, P.; Xu, J.; Boyer, C. Seeing the Light:  
5 Advancing Materials Chemistry through Photopolymerization. *Angew. Chem. Int.*  
6 *Ed.* 2019, 58, 5170-5189.  
7  
8
- 9  
10 15. Jung, K.; Xu, J.; Zetterlund, P. B.; Boyer, C. Visible-Light-Regulated  
11 Controlled/Living Radical Polymerization in Miniemulsion. *ACS Macro Lett.*  
12 2015, 4, 1139-1143.  
13  
14
- 15  
16 16. Jung, K.; Boyer, C.; Zetterlund, P. B. RAFT iniferter polymerization in  
17 miniemulsion using visible light. *Polym. Chem.*, 2017, 8, 3965-3970.  
18  
19
- 20  
21 17. Jasinski, F.; Zetterlund, P. B.; Braun, A. M.; Chemtob, A. Photopolymerization in  
22 dispersed systems. *Prog. Polym. Sci.* 2018, 84, 47-88.  
23  
24
- 25  
26 18. Qiao, L.; Zhou, M.; Shi, G.; Zhang, X.; Cui, Z.; Fu, P.; Liu, M.; Qiao, X.; He, Y.;  
27 Pang, X. Ultrafast Visible-Light-Induced ATRP in Aqueous Media with Carbon  
28 Quantum Dots as the Catalyst and Its Application for 3D Printing. *J. Am. Chem.*  
29 *Soc.* 2022, 144, 9817-9826.  
30  
31  
32  
33  
34  
35  
36  
37
- 38  
39 19. Jiang, J.; Ye, G.; Wang, Z.; Lu, Y.; Chen, J.; Matyjaszewski, K.  
40 Heteroatom-Doped Carbon Dots (CQDs) as a Class of Metal-Free Photocatalysts  
41 for PET-RAFT Polymerization under Visible Light and Sunlight. *Angew. Chem.*  
42 *Int. Ed.* 2018, 57, 12037-12042.  
43  
44  
45  
46  
47
- 48  
49 20. Kütahya, C.; Wang, P.; Li, S.; Liu, S.; Li, J.; Chen, Z.; Strehmel, B. Carbon Dots  
50 as a Promising Green Photocatalyst for Free Radical and ATRP-Based Radical  
51 Photopolymerization with Blue LEDs. *Angew. Chem. Int. Ed.* 2020, 59, 3166.  
52  
53  
54  
55
- 56  
57 21. Hao, Q.; Qiao, L.; Shi, G.; He, Y.; Cui, Z.; Fu, P.; Liu, M.; Qiao, X.; Pang, X.  
58 Effect of nitrogen type on carbon dot photocatalysts for visible-light-induced atom  
59  
60

- 1  
2  
3  
4 transfer radical polymerization. *Polym. Chem.* 2021, 12, 3060–3066.  
5  
6  
7 22. Fantin, M.; Isse, A. A.; Matyjaszewski, K.; Gennaro, A. ATRP in Water: Kinetic  
8  
9 Analysis of Active and Super-Active Catalysts for Enhanced Polymerization  
10  
11 Control. *Macromolecules* 2017, 50, 2696-2705.  
12  
13  
14 23. Fantin, M.; Isse, A. A.; Gennaro, A.; Matyjaszewski, K. Understanding the  
15  
16 Fundamentals of Aqueous ATRP and Defining Conditions for Better Control.  
17  
18 *Macromolecules* 2015, 48, 6862-6875.  
19  
20  
21  
22 24. Tannert, S.; Ermilov, E. A.; Vogel, J. O.; Choi, M. T. M.; Ng, D. K. P.; Röder, B.  
23  
24 The Influence of Solvent Polarity and Metalation on Energy and Electron Transfer  
25  
26 in Porphyrin-Phthalocyanine Heterotrimers. *J. Phys. Chem. B* 2007, 111,  
27  
28 8053–8062.  
29  
30  
31  
32 25. Fantin, M.; Chmielarz, P.; Wang, Y.; Lorandi, F.; Isse, A. A.; Gennaro, A.;  
33  
34 Matyjaszewski, K. Harnessing the Interaction between Surfactant and Hydrophilic  
35  
36 Catalyst To Control eATRP in Miniemulsion. *Macromolecules* 2017, 50,  
37  
38 3726–3732.  
39  
40  
41  
42  
43 26. Wang, X.; Cao, L.; Lu, F.; Mezziani, M. J.; Li, H.; Qi, G.; Zhou, B.; Harruff, B. A.;  
44  
45 Kermarrec, F.; Sun, Y.-P. Photoinduced electron transfers with carbon dots.  
46  
47 *Chem. Commun.* 2009, 3774–3776.  
48  
49  
50  
51 27. Zetterlund, P. B. Controlled/living radical polymerization in nanoreactors:  
52  
53 compartmentalization effects. *Polym. Chem.* 2011, 2, 534-549.  
54  
55  
56 28. Rolland, M.; Truong, N. P.; Parkatzidis, K.; Pilkington, E. H.; Torzynski, A. L.;  
57  
58 Style, R. W.; Dufresne, E. R.; Anastasaki, A. Shape-Controlled Nanoparticles  
59  
60

1  
2  
3  
4 from a Low-Energy Nanoemulsion. *JACS Au* 2021, 1, 11, 1975–1986.  
5

6 29. Rolland, M.; Dufresne, E. R.; Truong, N. P.; Anastasaki, A. The effect of  
7 surface-active statistical copolymers in low-energy miniemulsion and RAFT  
8 polymerization. *Polym. Chem.*, 2022,13, 5135-5144  
9  
10  
11  
12

13  
14 30. Bagheri, A.; Fellows, C. M.; Boyer C. Reversible Deactivation Radical  
15 Polymerization: From Polymer Network Synthesis to 3D Printing. *Adv. Sci.* 2021,  
16 8, 2003701.  
17  
18  
19  
20  
21  
22  
23  
24  
25  
26  
27  
28  
29  
30  
31  
32  
33  
34  
35  
36  
37  
38  
39  
40  
41  
42  
43  
44  
45  
46  
47  
48  
49  
50  
51  
52  
53  
54  
55  
56  
57  
58  
59  
60

For Table of Contents Use Only

